ATLAS Internal Note
MUON-NO-015
18 December 1992

A Simulation Study of Muon Reconstruction in the Air-Core Toroid

Andy Halley : Max Planck Institut für Physik, München

December 18, 1992

Abstract

The momentum response of the ATLAS Air-Core Muon System using High Pressure Drift Tubes has been simulated. Basic techniques are developed in order to study the various contributions to the total $\frac{\Delta p}{p}$ resolution of the system and to make comparisons with expectations.

1 Introduction

The air-core muon system response of ATLAS has been usefully parameterised as is presented in [1] and used as input to several physics analyses [2]. It is important to complement this with detailed studies of how such a performance may be realised in "reality". This is especially important when considering the issues of :

(i) Chamber resolutions and geometry,

(ii) Electromagnetic showers accompanying muons,

(iii) Mattress misalignment,

(iv) Energy losses and Landau tails,

(v) Algorithms and basic pattern recognition.

The purpose of this Note is to study these contributions at a preliminary level using a full GEANT simulation of the High Pressure Drift Tube (HPDT) Option in the Air-Core Toroid at a rapidity interval around $\eta \approx 0$.

Section 2 describes details of the simulation, particle tracking, reconstruction and simple pattern recognition before studying the various contributions to the total $\frac{\Delta p}{p}$ resolution in Section 3. The *reconstructed* muon momentum resolutions discussed in this Note are calculated as a function of muon momentum in Section 4 and compared to the *parameterised* resolutions of [1] used for earlier physics analyses.

2 Details of the Simulation

In order to study the muon resolution in detail, a simplistic test-beam geometry is employed. This is sketched in Figure 1. The geometry is essentially that of [3] with the simplifying assumptions that the transverse magnetic field is uniform and that muons are measured in the central azimuthal region, between two race-track [3] coils. The nominal dimensions [3] [4] are given in Table 1. The effects of material making up the inner tracking, calorimeters, coil and return yoke were estimated by placing a large (iron) absorber prior to the first muon station. The block's dimensions are determined by the sum of radiation lengths presented in Table 2.

Figure 1: Schematic of the simulated test-beam geometry.

Quantity	*Nominal Value*	*(Units)*
Magnetic field in the iron	0.0	T
Magnetic field before the toroid	0.2	T
Magnetic field in the air toroid	0.6	T
Equivalent iron thickness (115 X_0)	206	cm
Distance to first muon station	15	cm
Mattress superlayer separation	40	cm
Number of tube layers per superlayer	3	
HPDT wall thickness	200	μm
HPDT diameter	1	cm
Aluminium support plane thickness	300	μm
Separation between mattress centres	240	cm
Nominal coordinate resolution (per tube)	100	μm
Nominal mattress misalignment	100	μm

Table 1: Nominal dimensions and parameters of the simulated system. The magnetic field before the toroid is assumed to be purely azimuthal, ie. parallel to the toroidal field.

Sensitive layers (of air) were placed immediately behind the absorber to study the momentum and characteristics of EM shower particles leaking from the absorber into the muon system. Their absolute rates will be summarised briefly in a future Note [5].

As shown in Figure 1, a muon mattress consists of two *superlayers*, each made from 3 *layers* of aluminium HPDT's. These are supported in the same plane by aluminium plates on either

Source of Material	*Radiation Length (in X_0)*
Inner Tracking	0.25
Coil and Cryostat	1.00
Electromagnetic Calorimeter	27.00
Hadronic Calorimeter	87.44
Flux Return	0.11
Total	115.80

Table 2: Radiation length contributions of detectors prior to the muon system.

side of the mattress with similar plates placed vertically inside the mattress. The latter represent a negligible contribution to the amount of material traversed by particles in this study. The total amount of material in the muon system is given in Table 3. The geometry of the system is

Material	*Quantity*	*Density (g cm^3)*	X_0
Air	500 cm	0.00125	30420 cm
Tube Wall (Al)	$6 \times 2 \times 3 \times 200\mu m = 0.72$ cm	2.70	8.9 cm
Support Material (Al)	$0.3 \times 2 \times 3$ cm $= 1.8$ cm	2.70	8.9 cm

Table 3: Nominal materials present in the simulated muon system.

implemented in as flexible a way as possible with all dimensions, from the choice of tube radii to the mattress spacing, kept "floating" so that the component positions and dimensions of Table 1 are automatically recalculated on a run-by-run basis.

2.1 Particle Tracking

Single muons of momenta in the range 3 $\rightarrow$ 1 TeV/c are introduced into the system and tracked by GEANT, together with the products of any EM showers accompanying them. An additional complication is that, because of the small probability of interaction within a HPDT volume, muons are generally only tracked when entering and leaving a tube. Assuming single-hit electronics[1] the following procedure is adopted to calculate which particle triggered the measurement in a given tube :

- All shower particles, δ-rays etc are tracked inside the tube and the particle with closest approach to the central wire is selected.
- The traversing muon's input and exit points to the tube are used to give a projected point of closest approach. This approximation is valid for high momentum muons.
- The muon projection and closest "other" particle are compared and the particle with minimum distance is selected.

This algorithm is applied for each tube as a muon passes through the system.

2.2 Coordinate Resolution and Mattress Misalignment

The effects of the finite coordinate resolution of the HPDT's in the plane perpendicular to the magnetic field and the relative accuracy with which mattresses can be aligned are simulated in the following manner :

(a) Subsequent to the closest approach to the wire hit selection, the selected coordinate is smeared by a Gaussian with the nominal input resolution (see Table 1).

(b) In addition, for each event, the position of each mattress as a whole are also smeared according to a Gaussian with the nominal alignment precision.

In the latter, the alignment uncertainties are assumed to result in a *correlated* shift of the (maximal) 6 coordinates obtained from each mattress.

[1] As is done throughout this study.

2.3 Track Reconstruction

Tracks are reconstructed in the muon system using the following procedure :

(1) Basic pattern recognition - This is used to largely avoid shower particles in the innermost muon station confusing the helix fit. This is achieved by collecting hits in the *outermost* muon station and searching along a road in Z of variable width between the hits found there and the vertex. The uncertainty on the vertex is included in the road width calculation. Differing roads, of widths from $2 \rightarrow 5$ cm, give rise to identical results for muons of momenta $3 \rightarrow 1$ TeV/c whilst achieving a shower hit rejection of $\geq$ 90% depending on momenta.

(2) Helix fitting - A uniform field is assumed for the purposes of this study allowing a semi-analytical helix fit[2] to be employed. This algorithm is based on the formalism of Chernov and Ososkov [6] and allows an extremely fast and robust fitting procedure. By suitable choice of the minimisation parameter, it is also possible to fit helices with correlated displacements without previous knowledge of the coordinate errors such as those caused by mattress misalignment.

Hits are then selected for the track fit using the criterion of Sections 2.1 and 2.2 before being fed into the helix fitting algorithm. The resulting track helices are then used to calculate the $\frac{\Delta p}{p}$ resolution for muons exiting the iron absorber and entering the toroids.

3 Contributions to the Resolution

The total resolution in such a muon system can be thought of as the quadratic sum of several (largely) independent contributions. Their relative importance vary with the momentum of muon and may be listed as follows :

1. The smearing of muon momenta due to their passage through the inner detector material and subsequent energy loss fluctuations.
2. The effects of multiple scattering in the material of the mattresses and the HPDT's themselves.
3. The coordinate precision of the hit HPDT's making up the helix.
4. The uncertainty on the mattress positions.
5. The confusion caused by shower particles accompanying the muon.

The first and second of these considerations are more significant at low muon momenta, whereas the latter dominate at higher momenta. For many physics issues however, it is the region $\leq$ 100 GeV/c which is of importance for resolving signals in the presence of large backgrounds [2].

3.1 Energy Losses and Landau Tails

At muon momenta below 100 GeV/c, the relative contribution from energy losses in the detector material becomes more significant as the fraction of muons occupying the Landáu tail becomes greater. In this momentum region the $\frac{\Delta p}{p}$ response may best be described by the convolution of Landau and Gaussian distributions [1] where the width of the Landau is constrained to be *the same* as that of the Gaussian as shown in Figure 2. The fitting function used [1] is given by

[2] A code (HELFIT) is available from the author.

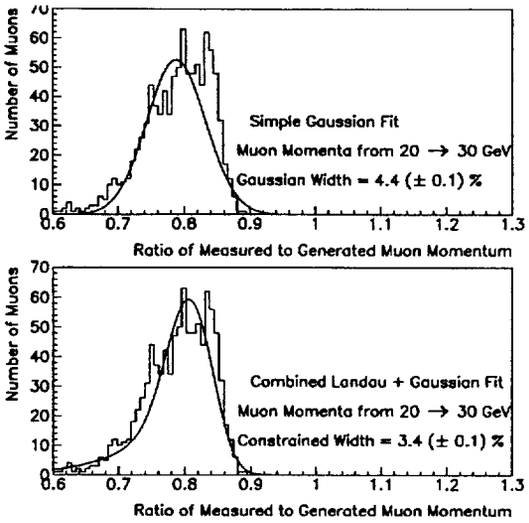

Figure 2: Comparison of simple Gaussian and a combined Landau *plus* Gaussian fit to muons of momenta in the range from 20 → 30 GeV/c. The *RMS* of the distribution shown, is 11% (if the histogram is not truncated) due to the long tails at lower values.

equation (1) :

$$F(p) = C_N C_L exp\left[-\left(\frac{p_0 - p}{\sigma} + e^{\frac{-p_0+p}{\sigma}}\right)/2\right] + C_N(1 - C_L)exp\left[\frac{-(p-p_0)^2}{2\sigma^2}\right] \qquad (1)$$

where; C_N is the normalisation factor, C_L is the relative Landau contribution, p_0 is the most likely value of reconstructed momentum and σ is the constrained *width* of the combined distribution. The relative contributions of the Landau and Gaussian terms vary with muon momentum, with the Landau contribution decreasing rapidly with momentum as shown in Figure 3. The Landau contribution can safely be neglected at muon momenta above $\approx$ 70 GeV/c. The *combined width* no longer has the same interpretation as the Gaussian width used in the parameterisations of [1]. In a sense it is more a mathematical construction. It is clear however that a single Gaussian fit is not sufficient, and tends to overestimate the measurement error at low muon momenta.

3.2 Multiple Scattering

The contribution from even relatively small quantities of material in the muon system can be relatively large. This is shown in Table 4. This is because even very small scatterings in the mattress material are significant when measurements are made over the long lever-arm of the system ($\approx$ 5 m). For example, the quantities of material shown in Table 2 reduce the radiation length of an hypothetical "all-air" system from 30,420 cm to 1670 cm.

The muon resolutions of Table 4 indicate that multiple scattering adds approximately 0.9% to the 0.6% resolution arising from energy losses of 100 GeV/c muons. The simulation results were cross-checked using the following numerical values calculated from [7] :

$$\text{Multiple scattering in 5 m of air} \Longrightarrow \frac{\Delta p}{p} = 0.2\%$$
$$\text{Multiple scattering in the muon system} \Longrightarrow \frac{\Delta p}{p} = 0.9\%$$

The simulated values to be compared to these are :

0.27 ($\pm$ 0.03)% and 0.90 ($\pm$ 0.03)% respectively.

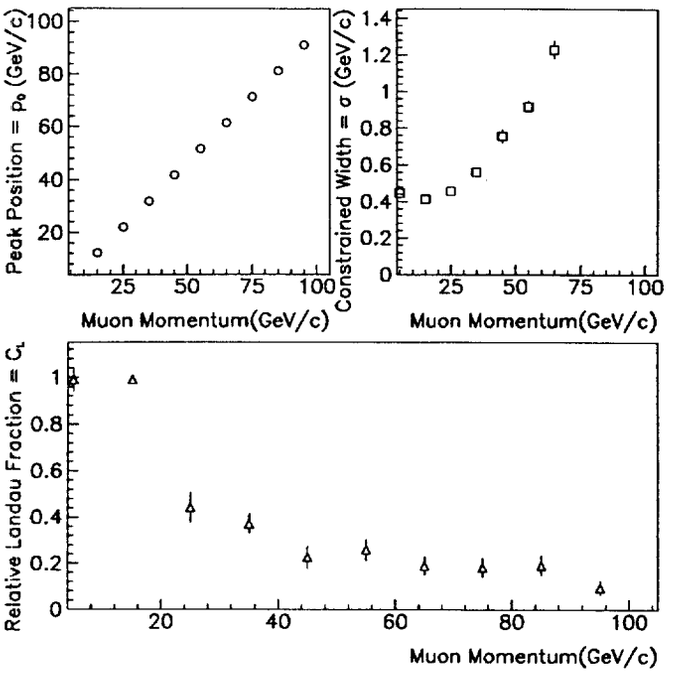

Figure 3: Variation of the combined fit parameters of equation (1) as a function of muon momentum.

These values are obtained using both the Gaussian and Moliere scattering options of GEANT [8] giving confidence in the stability of the results.

3.3 Pattern Recognition and Track Finding

At high momenta , muons passing through material radiate photons in a similar way to electrons at lower energies. This occurs during the muon's passage through the absorbing material prior to the muon system. Shower particles created within a critical distance from the absorber surface leak into the mattresses along with the muon. Simulation studies [9] [10] show that this critical distance is of the order of $t_{crit} \approx 20$ cm in iron. The extent to which this affects muon tracking depends on the distance and field between absorber and the first muon station'[11].

The effect of shower particles highlights the increasing need for (at least) primitive pattern recognition as the muon momenta increases. This is indicated by the number of "bad-fits" encountered when pattern recognition is not applied. This is illustrated in Figure 4.

3.4 Break-Down of Resolutions at 100 GeV/c

For example, in the case of a 100 GeV/c muon, the sum in quadrature and individually extracted resolution contributions are given in Table 4. At this muon momentum the contributions from Landau tails and EM shower particles are relatively small and it is the multiple scattering, HPDT and alignment accuracies which are of importance.

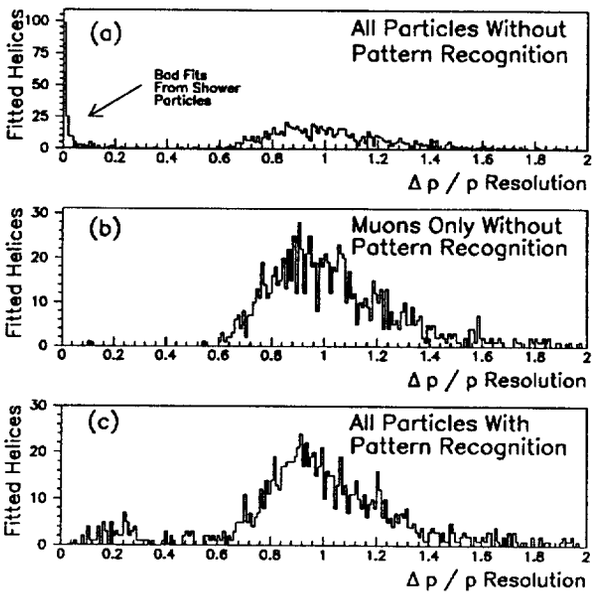

Figure 4: Illustration of the effects of shower particles on muon helix fits with (a) no pattern recognition, (b) no shower particles and (c) muons and shower particles *with* pattern recognition.

Momentum Smearing Mechanism	*Contribution to* $\frac{\Delta p}{p}$	*Cumulative Error*
Energy Loss Fluctuations	0.56 (± 0.02) %	0.56 (± 0.02) %
Multiple Scattering	0.96 (± 0.07) %	1.11 (± 0.06) %
HPDT Resolution	0.84 (± 0.13) %	1.39 (± 0.06) %
Mattress Alignment Uncertainty	1.91 (± 0.11) %	2.36 (± 0.08) %
Shower Particle Confusion in Helix Fit	0.31 (± 0.86) %	2.38 (± 0.08) %

Table 4: Contributions to the muon resolution at 100 GeV/c. The cumulative error correspond to assuming that all contributions are independent and may be added in quadrature.

4 Resolution Variation as a Function of Momentum

The resolutions around $\eta \approx 0$ may be divided into those in the ranges of muon momentum between 3 → 100 GeV/c and 100 GeV/c→1 TeV/c.[3] In the former, effects of multiple scattering and energy losses are significant whilst in the latter these are relatively small and increasing shower particle production and the detector precisions dominate.

The *reconstructed* resolutions are shown for the range of muons from 100 GeV/c→1 TeV/c in Figure 5 assuming the nominal detector parameters and precisions given in Table 1. In the momentum range below 100 GeV/c, care must be taken when dealing with Landau tails. The method adopted here is that of Section 3.1 where the fitting function of equation (1) is used to give a *constrained width* σ. This is compared to a simple Gaussian width in Figure 6.

[3]Higher momenta muons will be considered in future studies.

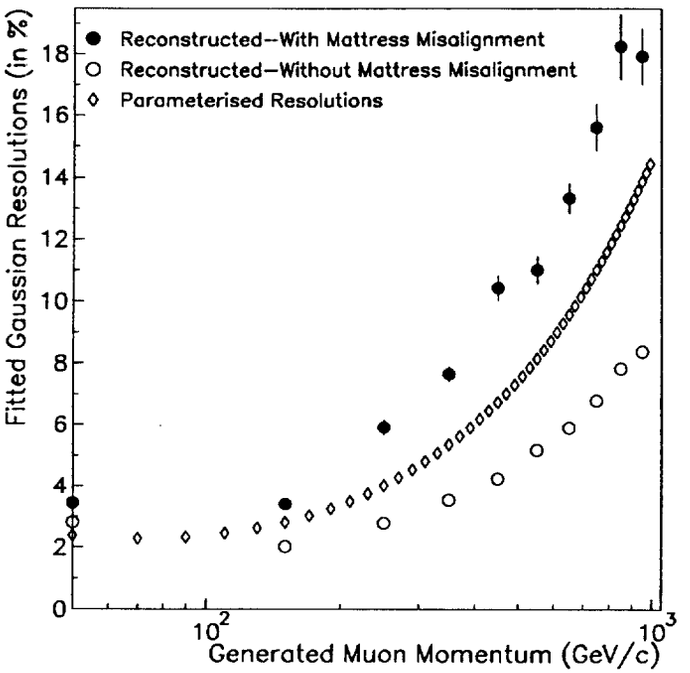

Figure 5: Muon resolution as a function of muon momenta (at the vertex) in the range from 100 GeV/c to 1 TeV/c assuming the detector precisions of Table 1. The Parameterised resolutions indicated refer to those used for physics simulations in [2].

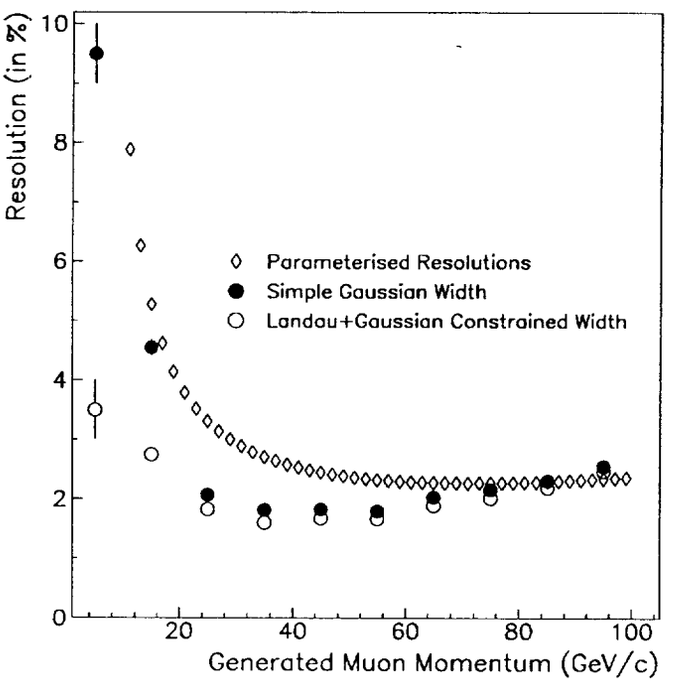

Figure 6: Reconstructed muon parameters as a function of muon momenta (at the vertex) in the range from 3 to 100 GeV/c assuming the detector precisions of Table 1. The *Parameterised* resolutions indicated refer to those used for physics simulations in [2] while the constrained widths refer to those of equation (1).

5 Conclusions

Simulations of the Air-Core muon system are instructive when considering the relative magnitude of contributions to the total $\frac{\Delta p}{p}$ resolution. As these vary with muon momenta, their interplay is crucial to understand the physics response of the detector and to develop reconstruction tools.

The muon response is studied in two momenta regions, above and below 100 GeV/c. A preliminary study of the influence of energy loss fluctuations indicates that such effects are significant below $\approx$ 30 GeV/c where symmetric $\frac{\Delta p}{p}$ distributions are no longer applicable. An immediate goal is to estimate the various contributions individually, as a function of muon momentum. Work is also continuing into utilising more realistic field maps over the full rapidity coverage. Systematic studies of the influences of :

- The non-uniform distribution of calorimeter and tracking material,
- An improved way of fitting the asymmetric $\frac{\Delta p}{p}$ distributions below 30 GeV/c,
- The effects of the azimuthal variation of the toroidal field,

are in progress.

6 Acknowledgements

I am indebted to Alexander Spiridonov for his work, and use of his parameterisations. I am also grateful to him and Karl Jakobs for helpful discussions and to Andrei Kriushin for extensive help and answering all of my stupid questions when using the UNIX systems at CERN.

References

[1] *"A Parameterisation of the Response Function of the Air-Core Toroid Muon System"*, A. Spiridonov et al, ASCOT/EAGLE Internal Note MU)-NO-008, 24 August 1992.

[2] *"Standalone Muon Performance for Intermediate Mass Higgs"*, R. St. Denis, ATLAS Internal Note PHYS-NO-011, 26 October 1992.

[3] ATLAS *Letter of Intent*, D. Gingrich et al, CERN/LHCC/92-4, 1 October 1992.

[4] Private communication with W. Blum.

[5] *"A Study of the Rates of EM Shower Particles from High Momentum Muons"*, A. Halley, (in preparation).

[6] N. Chernov amd N. Ososkov, Computer Physics Communications 33(1984) 329-333.

[7] *"Review of Particle Properties"*, The Particle Data Group, Physical Review D Number 11 Volume 45, 1 June 1992.

[8] "GEANT *User's Guide for Version 3"*, R. Brun et al, Data Handling Division Long Write-Up DD/EE/84-1, September 1987.

[9] Transparencies of Presentation to the ATLAS Muon Working Group Meeting on 4 November 1992 by the Author.

[10] Private communication with L. Nisati.

[11] *"Simulation of EM Showers from High Energy Muons (Status Report)"*, A. Halley, Transparencies presented to the ASCOT Workshop in CERN, 15 February 1992.